Multiple Access Capacity of UWB M-ary Impulse Radio Systems with Antenna Array

S. S. Tan, B. Kannan, *Member, IEEE*, and A. Nallanathan, *Senior Member, IEEE*

***Abstract*— In this paper, the multiple access capacity of an M-ary pulse position modulation (PPM) impulse radio (IR) system with antenna array is analyzed in dense multipath environments. An antenna array with Rake receivers is used to capture the signal energy from multipaths. Multiple access performance of the system is evaluated in terms of number of supported users for a given bit error rate and bit transmission rate with different number of antenna elements and selected paths. Numerical results show that the multiple access capacity of an M-ary IR system can be improved significantly by increasing the number of antenna elements and/or by adding more paths coherently at the receiver.**

***Index Terms*— Antenna array, impulse radio, M-ary, multiple access.**

I. Introduction

IMPULSE radio (IR) is a form of Ultra-wideband (UWB) spread spectrum signaling, which has properties that make it a suitable candidate for short range communications in dense multipath environments. Due to the large bandwidth, an IR multiple access system can accommodate many users. In [1], multiple access capability of a binary PPM IR system is studied with the assumptions of free space propagation conditions and additive white Gaussian noise. The authors in [2] investigate the use of M-ary equally correlated (EC) block waveform encoded PPM signals to increase the number of users supported by the system in free space propagation conditions. In multiuser environments with fading channels, antenna array can be used to exploit the spatial diversity in conjunction with the path diversity provided by the Rake receiver to capture the energy from different multipath components that are separated in space and time in a way that improve the performance of the system. In this paper, we present the multiple access performance of M-ary IR systems with antenna arrays in the presence of multipaths.

II. System Model

A typical time-hopping (TH) PPM signal for the u^{th} user can be modeled as

$$Y^{(u)}(t) = \sum_{i=0}^{\infty} \sum_{j=iN_s}^{(i+1)N_s-1} w(t - jT_f - c_j^{(u)}T_c - \delta^j_{d_i^{(u)}}) = \sum_{i=0}^{\infty} y^u_{i,d_i^{(u)}}(t), \quad (1)$$

Manuscript received October 8, 2003; revised November 24, 2004; accepted April 6, 2005. The associate editor coordinating the review of this letter and approving it for publication was A. Scaglione.

S. S. Tan and A. Nallanathan are with the Department of Electrical & Computer Engineering, National University of Singapore, 119260 (email: {engp2444, elena}@nus.edu.sg).

B. Kannan is with Institute for Infocomm Research, Heng Mui Keng Terrace, Singapore 119613 (email: kannanb@i2r.a-star.edu.sg).

Digital Object Identifier 10.1109/TWC.2006.01010

where $w(t)$ represents the monopulse (monocycle) waveform, T_f is the frame interval, T_c is the chip duration and $\delta^j_{d_i^{(u)}}$ $(1 \leq \delta^j_{d_i^{(u)}} \leq M)$ denotes the time shift for the data modulation. Each user is assigned a TH sequence, $\left\{c_j^{(u)}\right\}$ to support the multiple access capabilities. The i^{th} data symbol of the u^{th} user, $d_i^{(u)}$ is an M-ary symbol that conveys the information. The modulating data symbol changes only after every N_s hops, where N_s monopulses are transmitted per symbol. Hence, there are N_s frames in one symbol period, $T_s = N_sT_f$. The block waveform M-ary PPM signal set is $\{s_1(t), s_2(t), ...s_M(t)\}$, where $s_m(t)$ can be written as

$$s_m(t) = \sum_{j=0}^{N_s-1} w(t - jT_f - c_j^{(u)}T_c - \delta^j_m). \quad (2)$$

$$m = 1, 2, ...M.$$

In this paper, an M-ary EC signal is considered. In an M-ary EC signal, $\delta^j_m = a^j_m \tau_\delta \in \{0, \tau_\delta\}$, $a^j_m = \{0, 1\}$ [3], where τ_δ denotes the modulation index.

Energy of IR basic monopulse, E_w is denoted by $E_w = \int_{-\infty}^{\infty} w^2(t)\, dt$ and the corresponding normalized correlation function is defined as

$$\gamma_w(\tau_\delta) = \frac{1}{E_w} \int_{-\infty}^{\infty} w(t)w(t - \tau_\delta)\, dt. \quad (3)$$

Normalized correlation function [2] of the signals is defined as

$$\rho_{n,m} = \frac{1}{E_s} \int_{-\infty}^{\infty} y^{(u)}_{i,n}(t) y^{(u)}_{i,m}(t)\, dt \approx [1 + \gamma_w(\tau_\delta)]/2, \quad (4)$$

for $N_s \gg 1$ and $n \neq m$, where $E_s = E_b \log_2 M$ is the symbol energy and E_b is the bit energy. Note that for EC signals, $\rho_{n,m}(= \rho_{m,n}) = \rho$ when $n \neq m$ and $\rho_{n,m}(= \rho_{m,n}) = 1$ when $n = m$.

III. Application of Antenna Arrays in IR Systems

In this paper, we consider uniform rectangular $(A \times B)$ and linear $(A \times 1)$ arrays. The delay and sum beamformer is used to process the received signals at the array elements. The beamformer output for an array steered towards an azimuth angle of ϕ and an elevation angle of θ on incidence of a plane wave from an azimuth angle of ϕ_0 and an elevation angle of θ_0 is given by [4]

$$B(\phi, \theta, t) = \sum_{a=0}^{A-1} \sum_{b=0}^{B-1} a_{a,b}(\phi, \theta) \times w(t - \tau_{a,b}), \quad (5)$$

$$\tau_{a,b} = (a_c - a)\, \frac{d_x}{c}\, (u - u_0) + (b - b_c)\, \frac{d_y}{c}\, (v - v_0) \quad (6)$$

where $u = \sin\phi \sin\theta, u_0 = \sin\phi_0 \sin\theta_0, v = \cos\phi \sin\theta$, $v_0 = \cos\phi_0 \sin\theta_0$ and c is the speed of light. The spacing between antenna elements in x and y directions are denoted by d_x and d_y respectively. The antenna elements are equally spaced, where $d_x = d_y = 6$". The coordinate of the reference element is (a_c, b_c). The pattern of the $(a,b)^{th}$ element is denoted by $a_{a,b}(\phi,\theta)$. Each element is assumed to have an isotropic pattern and thus, $a_{a,b}(\phi,\theta)$ is equal to $1/(4\pi)$. Time delay of the received signal at the $(a,b)^{th}$ element is denoted by $\tau_{a,b}$, which is measured with respect to the reference element.

IV. Channel Model

The channel model is based on Saleh-Valenzuela (S-V) model with slight modifications [5]. Typically, the cluster decay factor (Γ) is larger than the ray decay factor (γ). We consider constant cluster arrival rate (Λ) and ray arrival rate (λ), where $\lambda > \Lambda$. We denote the arrival time of the p^{th} cluster by τ_p in which $p = 0, 1, 2, ...P-1$ and the arrival time of the q^{th} ray measured from the beginning of the p^{th} cluster by $\tau_{q,p}$, where $q = 0, 1, 2...Q-1$. The total number of clusters is P and the total number of rays within each cluster is Q. The total number of multipaths is $L_{total} = P \times Q$. The channel impulse response can be written as

$$\begin{aligned} h(t) &= \sum_{a=0}^{A-1}\sum_{b=0}^{B-1}\sum_{p=0}^{P-1}\sum_{q=0}^{Q-1} \alpha_{q,p,a,b}\delta\left(t-\tau_{a,b}-\tau_p-\tau_{q,p}\right) \\ &= \sum_{a=0}^{A-1}\sum_{b=0}^{B-1}\sum_{l=0}^{L_{total}-1} \alpha_{l,a,b}\delta\left(t-\tau_{l,a,b}\right), \qquad (7) \end{aligned}$$

where $\alpha_{q,p,a,b} \in \Re$, $\tau_{l,a,b} = \tau_{a,b} + \tau_p + \tau_{q,p}$ and $\delta(t)$ is the Dirac delta function. $\tau_{a,b}$ is defined in (6) and $\{\alpha_{q,p,a,b}\}$ is the gain coefficient of the q^{th} ray in the p^{th} cluster at the $(a,b)^{th}$ antenna element. Independent fading is assumed for each cluster, for each ray within the cluster and at each antenna element. The magnitudes of the channel gain follow a lognormal distribution where

$$\begin{aligned} &\alpha_{q,p,a,b} = \chi_{q,p,a,b}\xi_{p,a,b}\beta_{q,p,a,b} \qquad (8) \\ &20\log_{10}\left(\xi_{p,a,b}\beta_{q,p,a,b}\right) \propto Normal\left(\mu_{q,p,a,b}, \sigma_1^2+\sigma_2^2\right). \end{aligned}$$

In (8), $\xi_{p,a,b}$ is the fading associated with the p^{th} cluster at the $(a,b)^{th}$ antenna element, $\beta_{q,p,a,b}$ reflects the fading associated with the q^{th} ray within the p^{th} cluster at the $(a,b)^{th}$ antenna element and $\chi_{q,p,a,b}$ is the +/- sign with equal probability. The log value of each channel gain follows a normal distribution with mean $\mu_{q,p,a,b}$ and variance $\sigma_1^2+\sigma_2^2$, where σ_1^2 and σ_2^2 are respectively, the variance of the cluster lognormal fading and ray lognormal fading in dB. The normalized mean square value of $\alpha_{q,p,a,b}$ is defined as

$$\mathrm{E}\left[\alpha_{q,p,a,b}^2\right] = \Omega_0 e^{-\tau_{p,a,b}/\Gamma} e^{-\tau_{q,p,a,b}/\gamma}, \qquad (9)$$

where $\Omega_0 = \alpha_{q=0,p=0,a_c,b_c}^2 \Big/ \sum_{p=0}^{P-1}\sum_{q=0}^{Q-1}\alpha_{q,p,a_c,b_c}^2$ is the average power gain of the first ray of the first cluster for the reference element (a_c, b_c) which has been normalized by the total power gain of the reference element. The mean, $\mu_{q,p,a,b}$ is defined as

$$\begin{aligned} \mu_{q,p,a,b} &= \left[(10\ln(\Omega_0) - 10\tau_{p,a,b} - 10\tau_{q,p,a,b})/\ln(10)\right] \\ &\quad - \left[(\sigma_1^2+\sigma_2^2)\ln(10)/20\right]. \qquad (10) \end{aligned}$$

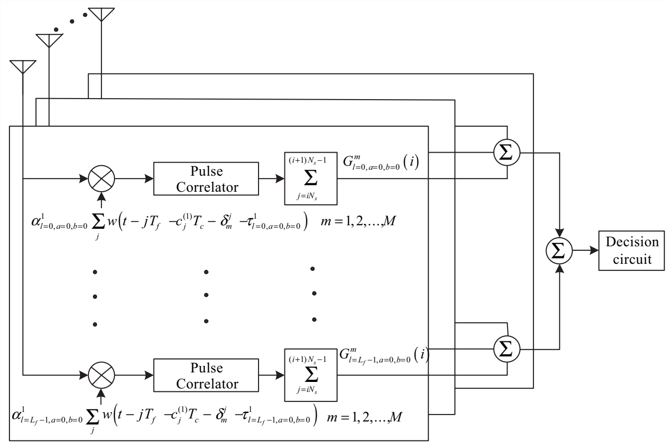

Fig. 1. Structure of SRake receiver with $(A \times B)$.

V. Receiver Processing

We use a Selective Rake (SRake) receiver with an antenna array and each antenna element has L_f Rake fingers as shown in Fig. 1, where the space-time correlators are used to process the received signals that are separated in space and time.

Without lost of generality, we assume that the receiver is perfectly synchronized to the hopping code of the desired user (user 1) and the delays of the selected paths are known at the receiver. The receiver selects the L_f^1 dominant paths of the user 1. The received signal can be written as

$$\begin{aligned} r(t) &= \sum_{a=0}^{A-1}\sum_{b=0}^{B-1}\sum_{l=0}^{L_f^1-1} \alpha_{l,a,b}^1 y_{i,d_i^{(1)}}^{(1)}(t-\tau_{l,a,b}^1) \\ &+ \underbrace{\sum_{a=0}^{A-1}\sum_{b=0}^{B-1}\sum_{l=L_f^1}^{L_{total}^1-1} \alpha_{l,a,b}^1 y_{i,d_i^{(1)}}^{(1)}(t-\tau_{l,a,b}^1)}_{n_{SI}(t)} \qquad (11) \\ &+ \underbrace{\sum_{u=2}^{N_u}\sum_{a=0}^{A-1}\sum_{b=0}^{B-1}\sum_{l=0}^{L_{total}^u-1} \alpha_{l,a,b}^u Y^u(t-\tau_{l,a,b}^u)}_{n_{MAI}(t)} + n_{a,b}(t), \end{aligned}$$

where $n_{SI}(t)$ and $n_{MAI}(t)$ denote the self interference (SI) and the multiple access interference (MAI), respectively. The AWGN noise at the $(a,b)^{th}$ element, $n_{a,b}(t)$ is with double-sided power spectral density of $N_0/2$. The notations $\tau_{l,a,b}^u$ and $\alpha_{l,a,b}^u$ are respectively, the time delay and the channel gain of the l^{th} path at the $(a,b)^{th}$ antenna element for the u^{th} user. An M-ary correlation receiver consists of M-filters matched to the signals $\left\{y_{i,m}^{(1)}(t-\tau_{l,a,b}^1)\right\}$, $m = 1, 2, ...M$. Test statistics of the transmitted symbols depend on the sum of the correlator outputs of each selected path at each antenna element.

VI. BER Analysis

The decision variable that is used in a binary test to decide between the signals pair, $y_{i,d_i^{(1)}=n}^{(1)}$ and $y_{i,d_i^{(1)}=m}^{(1)}$ is given by

$$G^{n,m}(i) = \sum_{a=0}^{A-1}\sum_{b=0}^{B-1}\sum_{l=0}^{L_f^1-1} G_{l,a,b}^{n,m}(i), \qquad (12)$$

$$G_{l,a,b}^{n,m} = \int_{t=iN_sT_f+\tau_{l,a,b}^1}^{(i+1)N_sT_f+\tau_{l,a,b}^1} \left(\alpha_{l,a,b}^1 y_{i,d_i^{(1)}}^1\left(t-\tau_{l,a,b}^1\right)\right)\alpha_{l,a,b}^1 v_{i,n,m}^1\left(t-\tau_{l,a,b}^1\right)dt + \underbrace{N_{SI}(t)+N_{MAI}(t)+N_{AWGN}(t)}_{N_{total}}, \quad (13)$$

$$N_{SI}(t) = \int_{t=iN_sT_f+\tau_{l,a,b}^1}^{(i+1)N_sT_f+\tau_{l,a,b}^1} \left(\sum_{l=0,l\neq l^{th}}^{L_{total}^1-1}\alpha_{l,a,b}^1 y_{i,d_i^{(1)}}^1\left(t-\tau_{l,a,b}^1\right)\right)\alpha_{l,a,b}^1 v_{i,n,m}^1\left(t-\tau_{l,a,b}^1\right)dt, \quad (14)$$

$$N_{MAI}(t) = \int_{t=iN_sT_f+\tau_{l,a,b}^1}^{(i+1)N_sT_f+\tau_{l,a,b}^1} \left(\sum_{u=2}^{N_u}\sum_{l=0}^{L_{total}^u-1}\alpha_{l,a,b}^u Y^u\left(t-\tau_{l,a,b}^u\right)\right)\alpha_{l,a,b}^1 v_{i,n,m}^1\left(t-\tau_{l,a,b}^1\right)dt, \quad (15)$$

$$N_{AWGN}(t) = \int_{t=iN_sT_f+\tau_{l,a,b}^1}^{(i+1)N_sT_f+\tau_{l,a,b}^1} n_{a,b}(t)\,\alpha_{l,a,b}^1 v_{i,n,m}^1\left(t-\tau_{l,a,b}^1\right)dt, \quad (16)$$

$$d_i^{(1)} \in \{m,n\} \text{ and } v_{i,n,m}^1(t) = \left[y_{i,n}^{(1)}(t) - y_{i,m}^{(1)}(t)\right]. \quad (17)$$

where $G_{l,a,b}^{n,m}(i)$ is defined in (13).

The conditional mean, $\Theta_{n,m}$ of the $G^{n,m}(i)$ is given by

$$\begin{aligned}\Theta_{n,m} &= E\left\{G^{n,m}(i)/d_i^{(1)}=n\right\} \\ &= (\sum_{a=0}^{A-1}\sum_{b=0}^{B-1}\sum_{l=0}^{L_f^1-1}(\alpha_{l,a,b}^1)^2)E_s(1-\rho_{n,m}). \quad (18)\end{aligned}$$

Furthermore, for EC signals,

$$\Theta_{n,m} = \begin{cases}\Theta = (\sum_{a=0}^{A-1}\sum_{b=0}^{B-1}\sum_{l=0}^{L_f^1-1}(\alpha_{l,a,b}^1)^2)E_s(1-\rho), & n\neq m \\ 0 & otherwise.\end{cases} \quad (19)$$

For an IR system in a multiuser environment, the transmission time difference between the l^{th} path of the user 1 at the $(a,b)^{th}$ element and the other paths from the same user or the other active users is defined as $\tau_{k,(a,b)}^u - \tau_{l,(a,b)}^1 = j_{k,l,(a,b)}^u T_f + q_{k,l,(a,b)}^u$, where $j_{k,l,(a,b)}^u$ is the time uncertainty rounded to the nearest integer, and $q_{k,l,(a,b)}^u$ is the error in this rounding process, which is assumed to be uniformly distributed over $[-T_f/2, T_f/2]$. In this paper, we assume that the number of users and the number of multipaths are sufficiently large. Hence, N_{MAI} and N_{SI} in (13) can be modeled as Gaussian random variables using the central limit theorem (CLT). Furthermore, N_{MAI} and N_{SI} can be considered as independent random variables as the user signals are all assumed to be independently generated. Therefore, N_{total} can be modeled by a Gaussian random variable with zero mean and σ_{total}^2 variance, where $\sigma_{total}^2 = \sigma_{SI}^2 + \sigma_{MAI}^2 + \sigma_{AWGN}^2$. The notations, σ_{SI}^2, σ_{MAI}^2 and σ_{AWGN}^2 are the variances of the decision variable caused by SI, MAI and AWGN respectively. The AWGN variance, σ_{AWGN}^2 can be written as

$$\sigma_{AWGN}^2 = \frac{N_0}{2}(\sum_{a=0}^{A-1}\sum_{b=0}^{B-1}\sum_{l=0}^{L_f^1-1}(\alpha_{l,a,b}^1)^2)\int_{-\infty}^{\infty}(v_{i,n,m}^1)^2(t)\,dt. \quad (20)$$

The variance, σ_{MAI}^2 can be written as

$$\sigma_{MAI}^2 = \quad (21)$$
$$\frac{N_s}{2T_f}\sum_{u=2}^{N_u}\sum_{a=0}^{A-1}\sum_{b=0}^{B-1}\sum_{l=0}^{L_f-1}\sum_{k=0}^{L_{total}^u-1}\left(\alpha_{l,(a,b)}^1\alpha_{k,(a,b)}^u\right)^2\int_{-\infty}^{\infty}R^2(x)\,dx,$$

where $R(\tau) = \int_{-\infty}^{\infty} w(t-\tau)[w(t)-w(t-\tau)]\,dt$. Similarly, the variance of decision variable caused by self interference, σ_{SI}^2 can be written as

$$\sigma_{SI}^2 = \quad (22)$$
$$\frac{N_s}{2T_f}\sum_{a=0}^{A-1}\sum_{b=0}^{B-1}\sum_{l=0}^{L_f-1}\sum_{k=0,(k\neq l)}^{L_{total}^1-1}\left(\alpha_{l,(a,b)}^1\alpha_{k,(a,b)}^1\right)^2\int_{-\infty}^{\infty}R^2(x)\,dx.$$

The union bound of the symbol error probability (SER) conditioned on a particular SNR can be written as

$$P_{s/\gamma}(N_u) = \frac{1}{M}\sum_{m=1}^{M}\sum_{n=1}^{M}Q\left(\sqrt{SNR^{n,m}(N_u)}\right), m\neq n. \quad (23)$$

From (18) and (19), the signal-to-noise ratio is defined by

$$\begin{aligned} & SNR^{n,m}(N_u) = (\Theta_{n,m})^2\Big/\sigma_{total}^2 = \Theta^2/\sigma_{total}^2 \\ = & \left[\left(\Theta^2/[\sigma_{AWGN}^2+\sigma_{SI}^2]\right)^{-1} + \left(\Theta^2/\sigma_{MAI}^2\right)^{-1}\right]^{-1} \\ = & SNR(N_u). \quad (24)\end{aligned}$$

Substituting (24) in (23), we obtain

$$P_{s/\gamma}(N_u) = (M-1)\,Q\left(\sqrt{SNR(N_u)}\right). \quad (25)$$

Corresponding upper bound of BER [3] can be written as

$$P_{b/\gamma}(N_u) = (M/2)\,Q\left(\sqrt{\log_2(M)\,SNRb(N_u)}\right). \quad (26)$$

$SNRb(N_u)$ in (26) is the output bit SNR and is defined by (27).

In (27), $\beta = 2\left[E_w\left((1-\gamma_w(\tau_\delta))/2\right)\right]^2\Big/\left[(1/T_f\int_{-\infty}^{\infty}R^2(x)dx\right]$, $R_b = \log_2(M)/N_sT_f$ is the bit transmission rate and

$$SNRb(N_u) = \left[(SNRb(1))^{-1} + \left(\frac{\left(\sum_{a=0}^{A-1} \sum_{b=0}^{B-1} \sum_{l=0}^{L_f^1 - 1} (\alpha_{l,a,b}^1)^2 \right)^2 \beta / T_f}{(R_b) \left(\sum_{u=2}^{N_u} \sum_{a=0}^{A-1} \sum_{b=0}^{B-1} \sum_{l=0}^{L_f - 1} \sum_{k=0}^{L_{total}^u - 1} \left(\alpha_{l,(a,b)^1} \alpha_{k,(a,b)}^u \right)^2 \right)} \right)^{-1} \right]^{-1} \quad (27)$$

$$D = \left[\left(\sum_{a=0}^{A-1} \sum_{b=0}^{B-1} \sum_{l=0}^{L_f^1 - 1} (\alpha_{l,a,b}^1)^2 \right)^2 \beta / T_f \right] \Big/ \sum_{u=2}^{N_u} \sum_{a=0}^{A-1} \sum_{b=0}^{B-1} \sum_{l=0}^{L_f - 1} \sum_{k=0}^{L_{total}^u - 1} \left(\alpha_{l,(a,b)}^1 \alpha_{k,(a,b)}^u \right)^2 \quad (31)$$

$SNRb(1)$ is the bit SNR of a single user system and is defined as

$$SNRb(1) = \log_2(M) \left[\Theta^2 / (\sigma_{AWGN}^2 + \sigma_{SI}^2) \right]. \quad (28)$$

The average BER, $P_b = E\left[P_{b/\gamma}(N_u)\right]$ is evaluated using Monte Carlo method.

VII. Degradation Factor and Multiple Access Capacity

Degradation factor is a measure of degradation in performance as the number of users with L_{total}^u paths increases. As in [3], $SNRb_s$ denotes the specified bit SNR to achieve the desired probability of error and $SNRb_r$ denotes the required value of $SNRb(1)$ to meet $SNRb(N_u) = SNRb_s$, where

$$SNRb_r(N_u) = \frac{SNRb_s}{1 - SNRb_s \left[(1/R_b)D\right]^{-1}}, \quad (29)$$

$$SNRb_s = \frac{SNRb_r(N_u)}{1 + SNRb_r(N_u) \left[(1/R_b)D\right]^{-1}}, \quad (30)$$

and D is given by (31). The degradation factor, DF is defined as

$$\begin{aligned} DF &= SNRb_r(N_u)/SNRb_s(1) \\ &= 1 \Big/ \left[1 - SNRb_s \left[(1/R_b)D\right]^{-1} \right]. \end{aligned} \quad (32)$$

From (32), we can get the bit transmission rate of R_b as

$$R_b(DF) = (1/SNRb_s)\left[1 - (1/DF)\right] D. \quad (33)$$

By using the Shannon capacity formula, we can derive the multiple-access channel capacity per user, $C_a(N_u)$ with antenna array at the receiver. The capacity formula is defined as

$$C(B) = B \log_2 \left(1 + (1/B) R_b SNRb_s(N_u)\right), \quad (34)$$

where $B = 1/T_w$ is the bandwidth of the signal with T_w as the duration of the monopulse.

For a given N_u, the $SNRb_s$ takes the maximum value when $SNRb_r(N_u) \to \infty$ in (30); i.e.,

$$SNRb_{\lim}(N_u) \triangleq \lim_{SNRb_r(N_u) \to \infty} SNRb_s = (1/R_b)D. \quad (35)$$

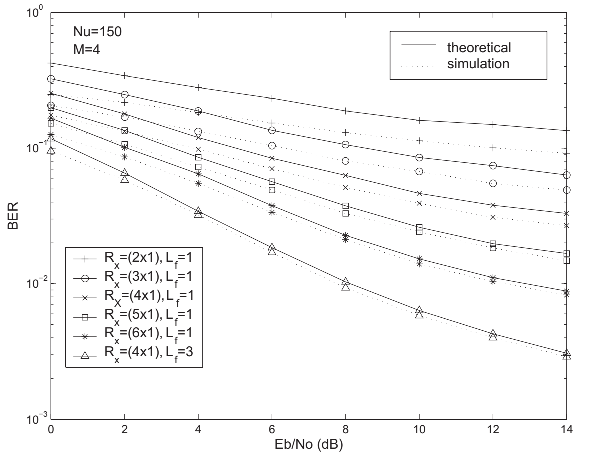

Fig. 2. The numerical bound and simulation results of IR system with different number of antenna elements and selected paths for a uniform linear array.

By substituting $SNRb_s(N_u)$ in (34) with $SNRb_{\lim}(N_u)$ and expanding (34) using the power series, the maximum value of $C(B)$ for a given B can be written as

$$C(B) = \left[B/\log_e 2\right] \sum_{k=1}^{\infty} \frac{(-1)^{k+1}}{k} \left[D/B\right]^k. \quad (36)$$

By setting $B \to \infty$, the multiple access capacity per user can be written as

$$C_a(N_u) \triangleq \lim_{B \to \infty} C(B) \approx D/\log_e(2). \quad (37)$$

VIII. Numerical Results

We consider a Gaussian monopulse, which is defined by

$$w(t) = \left(\left[1 - 4\pi\left((t - t_d)/\tau_m\right)^2\right] \exp\left[-2\pi\left((t - t_d)/\tau_m\right)^2\right] \right), \quad (38)$$

where $t_d = 0.35\,ns$ is the pulse center, and $\tau_m = 0.2877\,ns$ is the pulse width. In this paper, $T_f = 40\,ns$, $\tau_\delta = 0.156\,ns$, and the channel parameters, $\Gamma = 24$, $\gamma = 12$, $\sigma_1 = \sigma_2 = 3.3941\,dB$, $\lambda = 0.5/ns$ and $\Lambda = 0.1/ns$. The signals received at all antenna elements are assumed to be in phase, where $\phi = 15^0$, $\theta = 90^0$, $\phi_0 = 45^0$ and $\theta_0 = 90^0$. We assume

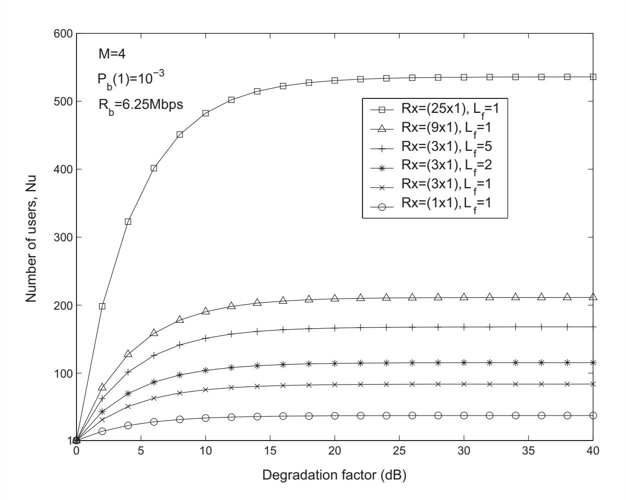

Fig. 3. Number of active users, N_u as a function of degradation factor with different number of antenna elements and selected paths for a uniform linear array.

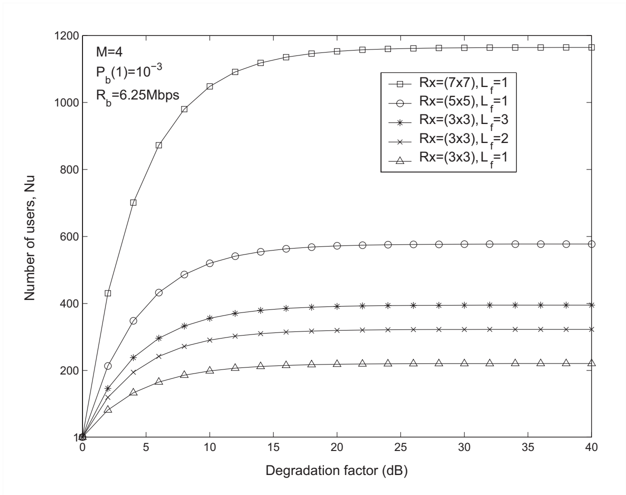

Fig. 4. Number of active users, N_u as a function of degradation factor with different number of antenna elements and selected paths for a rectangular planar array.

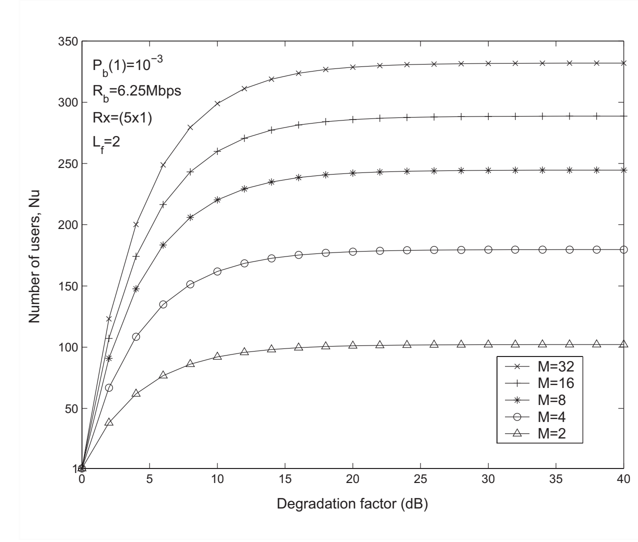

Fig. 5. Number of active users, N_u as a function of degradation factor for a uniform linear array of $Rx = (5 \times 1)$with $L_f = 2$ for different values of M.

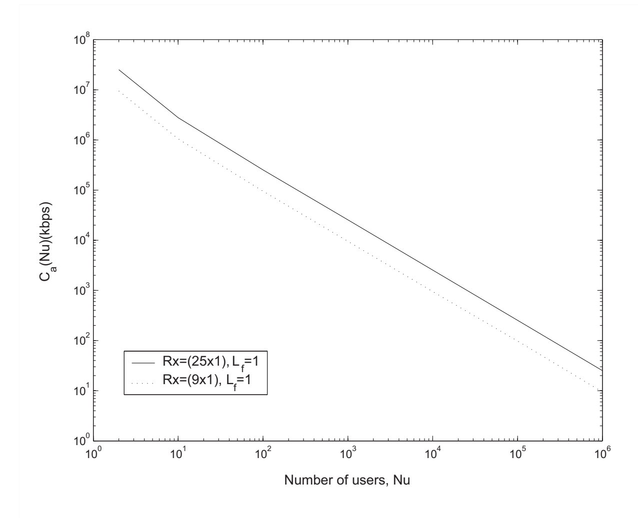

Fig. 6. The multiple access capacity per user $C_a(N_u)$ as a function of number of active users N_u for $Rx = (9 \times 1), (25 \times 1)$ elements of a uniform linear array with $L_f = 1$.

$L_{total}^u = L_{total} = 20$. The number of pulses in one symbol, $N_s = \log_2(M)\, N_s^b$ where N_s^b is the number of pulses used in binary communications and is set to 4 in this paper.

Fig. 2 shows the theoretical and simulation results of the system's BER performance for different number of antenna elements and selected paths. Theoretical and simulation results match reasonably well. The figure also shows that the BER of an M-ary system improves with increasing number of antenna elements and/or with increasing number of selected paths.

Fig. 3 and Fig. 4 show the effect of number of selected paths and antenna elements on the multiple access performance of the system with uniform linear and rectangular arrays, respectively. One can observe from these two figures that the number of simultaneous users supported by the system increases with increasing number of antenna elements and/or with increasing number of selected paths. It allows one to capture more multipath signal energy and hence, to enhance the multiple access capability of the system.

Fig. 5 shows the effect of M on the multiple access performance of the system with a uniform linear array. This figure shows that it is possible to increase the number of supported users, without increasing each user's signal power, by increasing the value of M.

Fig. 6 shows the multiple access capacity per user $C_a(N_u)$ as a function of number of users. This figure suggests that the multiple access capacity per user of an IR system can be improved by increasing the antenna elements.

IX. Conclusions

In this paper, the multiple access performances of M-ary IR systems with antenna arrays in multipath environments are presented. Antenna array can be used in conjunction with the Rake receiver to increase the multiple access capability. The results indicate that the multiple access capacity of an

IR system improves significantly when the number of the antenna elements and/or selected paths at the receiver is increased. However, increasing the antenna elements and/or selecting more paths will increase the complexity of a receiver. Therefore, a system designer has to decide a suitable number of antenna elements and/or the multipaths in order to achieve the required multiple access capacity.

REFERENCES

[1] R. A. Scholtz, "Multiple access with time hopping modulation," in *Proc. IEEE MILCOM '93*, pp. 447-450, Oct. 1993.

[2] F. Ramirez-Mireles and R. A. Scholtz, "Multiple-access with time hopping and block waveform PPM modulation," in *Proc. IEEE ICC '98*, vol. 3, pp. 775-779, June 1998.

[3] F. Ramirez-Mireles, "Performance of ultra wideband SSMA using time hopping and M-ary PPM," *IEEE J. Select. Areas Commun.*, vol. 19, pp. 1186-1196, June 2001.

[4] R. J. -M. Cramer, M. Z. Win, and R. A. Scholtz, "Impulse radio multipath characteristics and diversity reception," in *Proc. IEEE ICC '98*, vol. 3, pp. 1650-1654, June 1998.

[5] A. F. Molisch, J. R. Foerster, and M. Pendergrass, "Channel models for ultrawideband personal area networks," *IEEE Pers. Commun.*, vol. 10, pp. 14-21, Dec. 2003.